

# The Different T-cell Receptor Repertoires in Breast Cancer Tumors, Draining Lymph Nodes, and Adjacent Tissues

Ting Wang<sup>1</sup>, Changxi Wang<sup>2</sup>, Jinghua Wu<sup>2</sup>, Chenyang He<sup>1</sup>, Wei Zhang<sup>2</sup>, Jiayun Liu<sup>3</sup>, Ruifang Zhang<sup>2</sup>, Yonggang Lv<sup>1</sup>, Yongping Li<sup>1</sup>, Xiaojing Zeng<sup>2</sup>, Hongzhi Cao<sup>2</sup>, Xiuqing Zhang<sup>2</sup>, Xun Xu<sup>2</sup>, Chen Huang<sup>4</sup>, Ling Wang<sup>1</sup>, and Xiao Liu<sup>2,5</sup>

## Abstract

T lymphocytes infiltrate the microenvironment of breast cancer tumors and play a pivotal role in tumor immune surveillance. Relationships between the T-cell receptors (TCR) borne by T cells within tumors, in the surrounding tissues, and in draining lymph nodes are largely unexplored in human breast cancer. Consequently, information about the relative extent of possible T-cell exchange between these tissues is also lacking. Here, we have analyzed the TCR repertoire of T cells using multiplex PCR and high-throughput sequencing of the TCR $\beta$  chain in the tissues of tumor, adjacent nontumor, and axillary lymph nodes of breast cancer patients. T-cell repertoire diversity in tumors was lower than in lymph nodes, but higher than in nontumor tissue, with a

preferential use of variable and joining genes. These data are consistent with the hypothesis that most of the T cells in tumors derive from the lymph node, followed by their expansion in tumor tissue. Positive nodes appeared to enhance T-cell infiltration into tumors and T-cell clonal expansion in lymph nodes. Additionally, the similarity in TCR repertoire between tumor and nontumor tissue was significantly higher in luminal-like, rather than basal-like, breast cancer. Our study elucidated the high heterogeneity of the TCR repertoire and provides potential for future improvements in immune-related diagnosis, therapy, and prognosis for breast cancer patients. *Cancer Immunol Res*; 5(2); 1–9. ©2016 AACR.

## Introduction

Tumorigenesis is regulated by immune responses to neoantigens in the tumor microenvironment, including the plasticity of macrophage (1) and suppression of antitumor immune response (2, 3). More than a decade ago, Schreiber proposed the three "E roles" (elimination, equilibrium, and escape) of immune surveillance, which interprets the interaction between tumor and host immune system in tumor progression (4). Lymphocytes are the major antitumor cells in tumor microenvironments, and many studies have demonstrated that tumor-infiltrating lymphocytes (TILs), especially CD8<sup>+</sup> T cells, are related to improved clinical prognosis in most of the tumor types (5), such as ovarian cancer (6), cervical cancer (7),

colorectal cancer (8–10), and breast cancer (11–14). The presence and antitumor function of TILs makes cures of tumor by immunotherapy possible (15, 16).

To counteract tumor-induced immunosuppressive microenvironments, several immunotherapy strategies have been developed to enhance the antitumor immune response. Adoptive cell transfer (ACT) is one such strategy, which depends directly on the presence of antitumor T cells, by treating the patients with T cells isolated from the tumor mass and expanded *ex vivo* (15). Immunotherapies based on the adoptive transfer of TILs have had surprisingly positive results for some patients with metastatic melanoma (16). Another immunotherapeutic strategy directly relying on the existence of TILs is immune checkpoint blockade, which inhibits the interaction of cytotoxic T lymphocyte antigen 4 (CTLA-4) or programmed cell death 1 receptor (PD-1) with their ligands using blocking antibodies. Immune checkpoint blockade can activate the T cells in the microenvironment and has led to durable antitumor effects in patients with metastatic melanoma (17, 18), renal cell carcinoma, and non-small cell lung cancer (18). Checkpoint blockade had such therapeutic efficacy for various types of cancer, that cancer immunotherapy was chosen by the editors of *Science* as the biggest scientific breakthrough of 2013. However, current immunotherapies do not work for every patient, emphasizing the need to further understand and monitor the infiltrating T cells in cancer.

Breast cancer is the second leading cause of cancer death among women in the United States (19) and has become one of the most lethal diseases worldwide. Infiltrating lymphocytes are an independent prognostic factor associated with better breast

<sup>1</sup>Department of Vascular and Endocrine Surgery, Xijing Hospital, Fourth Military Medical University, Xi'an, China. <sup>2</sup>BGI-Shenzhen, Shenzhen, China. <sup>3</sup>Institute of Clinical Laboratory Medicine, Xijing Hospital, Fourth Military Medical University, Xi'an, Shaanxi, China. <sup>4</sup>Department of Nephrology, Xijing Hospital, Fourth Military Medical University, Xi'an, Shaanxi, China. <sup>5</sup>Department of Biology, University of Copenhagen, Copenhagen, Denmark.

**Note:** Supplementary data for this article are available at Cancer Immunology Research Online (<http://cancerimmunolres.aacrjournals.org/>).

T. Wang, C. Wang, J. Wu, and C. He contributed equally to this article.

**Corresponding Authors:** Xiao Liu, BGI-Shenzhen, Build 11, Beishan Industrial Zone, Yantian District, Shenzhen, China. Phone: 86-13428700710; Fax: 86-0755-36307273; E-mail: liuxiao@genomics.cn; and Ling Wang, vascular@fmmu.edu.cn

**doi:** 10.1158/2326-6066.CIR-16-0107

©2016 American Association for Cancer Research.

cancer patient survival. Recently, next-generation sequencing has been utilized to investigate the T-cell receptor (TCR) repertoire of infiltrating T lymphocyte in renal cell carcinoma (19) and ovarian cancer (20), but not in breast cancer. The clonal diversity of infiltrating lymphocytes in breast tumor tissues, and its comparison with that of adjacent tissues, remains largely unexplored.

The tumor-draining lymph nodes (LN) are the LNs that lie immediately downstream of tumors, and for breast cancer, axillary LNs are the most important draining LNs that provide significant diagnostic and prognostic value. The degree of overlap of TCR repertoire between the tumor tissue and draining LNs can be used to assess the percentage of infiltrating T cells derived from draining LNs (21). Therefore, we have also investigated the derivation of tumor-infiltrating T cells by comparing the TCR repertoire of tumor-infiltrating T cells with that of breast-draining LN T cells from the same breast cancer patient.

It is reported that the association of TILs with clinical outcome is observed just in basal-like or triple-negative breast cancer, but not in luminal breast cancer (13). One previous study has shown that basal type breast cancer cell lines express more PD-L1 compared with luminal breast cancer cell lines (22). Therefore, it is possible that the TILs in luminal breast cancer are different from those in basal-like breast cancer. Comparing the TCR repertoire of infiltrating T cells of the luminal breast cancer with that of the basal breast cancer can help verify this hypothesis. The shared (public) TCRs observed in multiple individuals, and their association with disease antigens, such as tumor neoantigens, have been investigated for decades (23, 24). Recombinational biases and convergent recombination are proposed to contribute to the occurrence of public TCRs (23). In this study, we present the public intratumoral TCRs for breast cancer and incorporate this information in our explanation of the contributions of different mechanisms.

Overall, in this study, we attempt to (i) assess the amount of T-cell infiltration and TCR diversity of adjacent tissues; (ii) investigate the percentage of tumor-infiltrating T cells that were derived from draining LN; (iii) uncover associations between the TCR repertoire and other clinical features, including node positivity and tumor subtypes; and (iv) characterize public TCR response among breast tumors. The results we present could help us to better understand the infiltrating T lymphocytes in

breast cancer, be beneficial in the effective design and better monitoring of breast cancer immunotherapy, and allow the improved stratification of the patients for treatment and outcome prediction.

## Materials and Methods

### Clinical samples

This study is based mainly on analyses of 16 female breast cancer patients from Xijing Hospital, the Fourth Military Medical University, China. All the tissues were treatment naïve and were removed during surgery of the patients who had not experienced any chemotherapy. The study was approved by the Institutional Review Board of Xijing Hospital and BGI-Shenzhen. Written informed consents were obtained from every participant. The clinical information of these patients was shown in Table 1. The 16 patients can be divided into two subgroups (8 in luminal type and the other 8 in nonluminal type) according to the expressions of estrogen receptor (ER), progesterone receptor (PR), human epidermal growth factor receptor 2 (Her2), and Ki-67 protein (see below).

Cancer tissue, normal breast tissue, and the draining LN (axillary LN) were collected during the surgery. Spatially different tumor specimens were collected and combined to be more representative of the tumor tissue. All of the solid specimens were cut into small pieces (1 mm<sup>3</sup>) immediately after surgery and transferred into a 2-mL freezing tube with preservation solution (RPMI 1640 with 15% fetal calf serum and 10% DMSO). After immersion in liquid nitrogen for 30 minutes, the samples were placed in -80°C for long-term storage. High-quality genomic DNA (gDNA) was extracted from frozen tissues by the common salting-out method.

Additionally, 20 breast tumor tissues were selected from the tissue repository in the Xijing Hospital, in which 14 were node-positive tumors with LN ratio [the number of positive LNs (pLN) divided by the number of LNs removed during surgery] of more than 50%, and six were node-negative tumors. These tissues were combined with the 16 tumors for analysis, to validate the association between tumor infiltration rate and node positivity. TCR repertoire data from another independent cohort of 49 patients, who had been consecutively recruited in year 2013 in Xijing Hospital, were used for validation (data not published), to

**Table 1.** The pathological data of the discovery cohort in the study

Patient ID	ER	HER2	PR	Ki-67	Lymph node ratio	Tumor subtype	Tumor infiltration (%)	Nontumor infiltration (%)
BC0001A	3+	-	2+	20%	0/16	Luminal B	NA	NA
BC0002A	1+	+	-	35%	0/6	Luminal B	10	2
BC0003A	-	-	-	30%	1/14	Basal-like	20	0.1
BC0004A	3+	-	3+	10%	0/16	Luminal A	8	1
BC0005A	3+	+	2+	5%	1/18	Luminal B	0.3	0.1
BC0006A	-	-	-	95%	0/5	Basal-like	25	0.5
BC0007A	-	-	-	20%	0/23	Basal-like	2	1
BC0008A	-	+	-	40%	0/29	HER2 enriched	NA	NA
BC0009A	1+	-	-	30%	14/18	Luminal B	30	0.1
BC0010A	-	-	-	50%	15/15	Basal-like	40	0.2
BC0011A	3+	-	2+	5%	0/20	Luminal A	8	0.1
BC0012A	2+	+	1+	28%	0/16	Luminal B	3	1
BC0013A	-	-	-	50%	0/18	Basal-like	2	0.2
BC0014A	3+	-	3+	28%	0/23	Luminal B	0.2	2
BC0015A	-	-	-	60%	0/5	Basal-like	15	3
BC0016A	3+	-	2+	10%	1/10	Luminal A	12	0.1

NOTE: NA means this sample was not analyzed.

compensate for the limited sample size and statistical power in our discovery cohort, for some of the analyses. These tissues were also treatment naïve and were representative of the hospitalized patients in that period. Samples from this cohort were collected following the same protocol described above.

### IHC and molecular subtype of patients

Molecular subtypes of breast cancer were classified according to the expression of ER, PR, HER2, and Ki-67, detected by IHC stained methods. Luminal A was defined as ER<sup>+</sup> and/or PR<sup>+</sup>, HER2<sup>-</sup>, Ki-67 less than 14%; luminal B was defined as ER<sup>+</sup> and/or PR<sup>+</sup>, HER2<sup>+</sup> or HER2<sup>-</sup>, and Ki-67 more than 14%; HER2 was defined as ER<sup>-</sup>, PR<sup>-</sup>, and HER2<sup>+</sup>; and triple-negative (TNP) or basal-like subgroup was defined as ER<sup>-</sup>, PR<sup>-</sup>, and HER2<sup>-</sup> (25).

### Infiltrating T-lymphocyte quantification

The T lymphocytes infiltrating in tumor and adjacent nontumor tissues were analyzed by IHC using antibody against human CD3, CD4, and CD8 based on formalin-fixed paraffin-embedded slides. Stained slides were scored and quantified by digital scanning. Positive T lymphocytes were visually scored by a pathologist who was blind to the clinical characteristics of the patients. Tumor-infiltrating T lymphocytes were defined as CD3<sup>+</sup> cells in tumor tissues, including those located within tumor cell nests and in the adjacent peritumoral stroma. The percentage of T lymphocytes infiltrating was calculated by dividing the number of total nucleated cells by the CD3<sup>+</sup> cells. To assess the reproducibility and reliability of the scoring, all cases were scored again by the same pathologist after a period of time (4 weeks) and were re-scored by a second pathologist. Both the scorings of the same pathologist, and from the two pathologists, showed very high reproducibility (Supplementary Table S1). We used Pearson correlation analysis to represent the reproducibility of the same pathologist, and the coefficient was 0.996. The intraclass correlation (ICC) is a better indicator to show the reproducibility between two pathologists, and the ICC consistency of our data was 0.986.

### High-throughput sequencing and analysis of TCR repertoire

The third complementary determining region (CDR3) of TCRs was amplified by multiplex PCR and sequenced using methods described previously (26–28). Briefly, gDNA (1,500 ng) for each sample was amplified using the QIAGEN Multiplex PCR Kit (QIAGEN) with 32 forward primers annealed to the FR3 region and 13 reverse primers annealed to the junction (J) region of TCR published in our previous study (29). The reaction cycling conditions were: 95°C 15 minutes, 30 cycles of 30 seconds at 94°C, 90 seconds at 60°C, and 30 seconds at 72°C, plus a final extension of 5 minutes at 72°C. The primers and multiplex PCR reaction have been optimized to minimize the multiplex PCR bias before the beginning of the study, and the bias has been assessed using the synthetic templates (Supplementary Fig. S1). The target amplified product (100–200 bp) was purified by electrophoresis on 2% agarose gel and then were sequenced with standard 2 × 150 paired-end reads on the Illumina HiSeq2000 platform.

Sequencing data were analyzed by an in-house developed pipeline *IMonitor* (29). A brief summary of the pipeline is as follows: (i) The low-quality reads and badly adapter contaminated reads were filtered to get clean reads. (ii) The cleaned pair-end reads were merged, and the reads that could not be merged were

discarded. (iii) The merged reads were aligned to their respective V, D, J germline sequences (IMGT, <http://www.imgt.org/>) using BLAST. (iv) Realignment of the correctly mapped reads was performed to select the best V/D/J alignment.

### Statistical analyses

To study the distribution of the *TRBV* and *TRBJ* genes of these three tissues of breast cancer patients, pairwise V-segment and J-segment profile comparisons were performed between tumor and other tissues. Because V gene frequencies are not all independent, we used a permutation test based on the Mann–Whitney *U* statistics (Shuffled-*U* Test; ref. 30). The resulting *P* values were corrected for multiple testing using false discovery rates. Statistical significance for the difference between two groups in other analyses were all determined using the Mann–Whitney *U* test. A paired test was used in case samples from the same patient were compared. For calculation of the Shannon diversity index, we included the top 1,000 unique clones to minimize the effect of sequencing errors. A *P* value lower than 0.05 was considered statistically significant. All analyses were performed with R version 3.0.2.

### Data availability

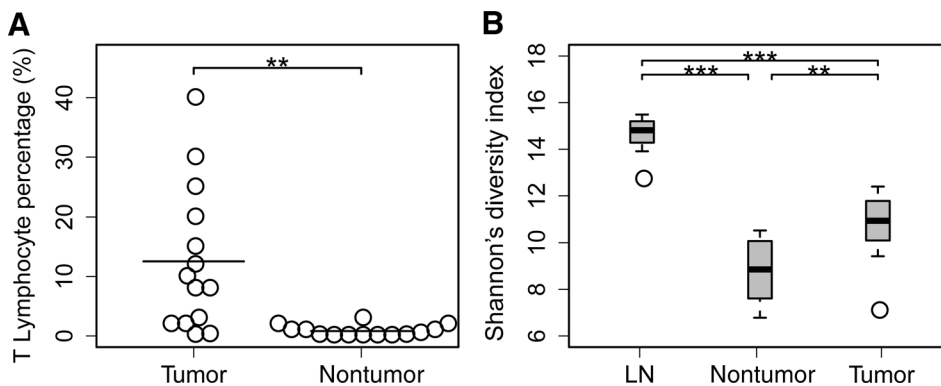
The raw sequence data of the TCR repertoire from the 16 patients have been deposited at the NCBI Sequence Read Archive (SRA) under the accession number SRA455606. Besides, we have uploaded all processed CDR3 sequences analyzed in this article to a public database (Pan Immune Repertoire Database, PIRD, [http://db.cngb.org/pird/breast\\_cancer\\_research](http://db.cngb.org/pird/breast_cancer_research)), which facilitates sequences query, comparison, and further analysis.

## Results

### Comparison of TCR diversity and gene usage between tumors and adjacent tissues

IHC staining and careful scoring of the T lymphocytes in the tissues revealed that the proportion of infiltrated T lymphocytes into the tumor microenvironment varied considerably among tumors and adjacent nontumor tissues (Table 1). Overall, breast tumors exhibited a significantly higher extent of T-lymphocyte infiltration than their paired nontumor tissues ( $P = 0.0023$ , Fig. 1A). The CD4<sup>+</sup> and CD8<sup>+</sup> T cells in tumors and nontumors were also analyzed (Supplementary Table S2).

Genomic DNA from the three types of tissues was used to profile the TCR  $\beta$  chain by high-throughput sequencing. The abundantly diversified *TRB* CDR3 sequences, which were unlikely to be shared by two unrelated T cells, served as unique barcodes for the T lymphocytes. We first evaluated the diversity of T cells in the neighboring tissues. The Shannon diversity index was used to calculate T-cell diversity (29). The T-cell population that had infiltrated tumors was significantly less diverse than that in LN ( $P = 6.104 \times 10^{-5}$ ; Fig. 1B, LN stated here and in the following refers to draining LN), but were more diversified than the matched nontumor tissue ( $P = 1.825 \times 10^{-2}$ ). The diversity of T lymphocytes in nontumor tissue was significantly lower than in LN ( $P = 1.526 \times 10^{-4}$ ) and varied extensively among individuals (Fig. 1B). We also calculated the curve of cumulative frequency of total clones with cumulative unique clones (Supplementary Fig. S2A) and the proportion of the abundant TCR clones ( $> 0.01\%$ ; Supplementary Fig. S2B).

**Figure 1.**

Proportion and diversity of infiltrated T lymphocytes in breast tumor and other tissues. **A**, Comparison of infiltration proportion of T lymphocytes in tumor and nontumor breast tissue of 14 patient samples analyzed by IHC ( $P = 0.0023$ ). **B**, Shannon diversity index of LN, nontumor, and tumor tissue. \* $p < 0.01$ , \*\*\* $p < 0.001$  according to Mann-Whitney U test.

The above two indexes demonstrated the same trends, with TCR repertoire diversity in nontumor < in tumor < in LN.

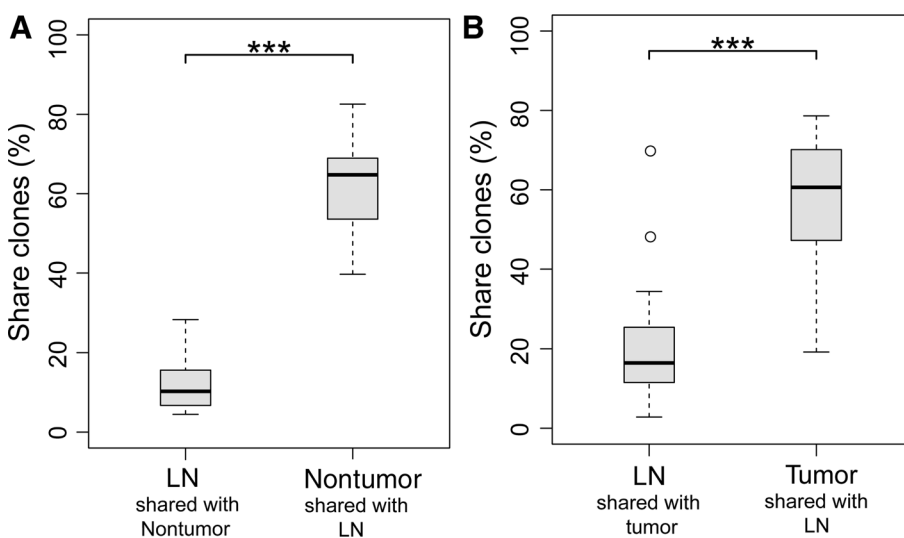
To further explore the properties of infiltrated T cells in tumors, we compared the *TRBV* and *TRBJ* gene usage of TCR repertoire in tumor tissue with matched LNs and nontumors. We tested all the V and J gene usage frequencies and identified the biased usage of J1-1, J1-6, J2-7, and J2-4 of J genes, between tumor and LN. Only the V24-1 gene usage discrepancy was observed between tumor and nontumor (Supplementary Fig. S3). The differences between tumor and other tissue implied the unique V or J usage pattern for TCR in tumors.

#### Most tumor-infiltrated T lymphocytes detected in draining LNs and expanded in tumors

Draining LNs serve as a T-lymphocyte reservoir that includes both naïve and activated lymphocytes, where transferred tumor antigens are presented by antigen-presenting cells to naïve T lymphocytes that become activated if they recognize the antigen. We had a unique opportunity to characterize the T cells that underwent this process by comparing the *TRB* CDR3s among the tumor and related tissues. Specifically, we found that about 60% of CDR3 rearrangements in tumor samples could be tracked in matched LNs, whereas only 10% to 20% of CDR3 rearrangements in the LNs were found in tumor samples. The similar ratio could also be found between adjacent non-

tumor samples and LNs (Fig. 2). The high proportion of CDR3s in tumor and normal samples that corresponds to LNs suggests that draining LNs provide a major source for the T-cell infiltration in tumor and normal tissues.

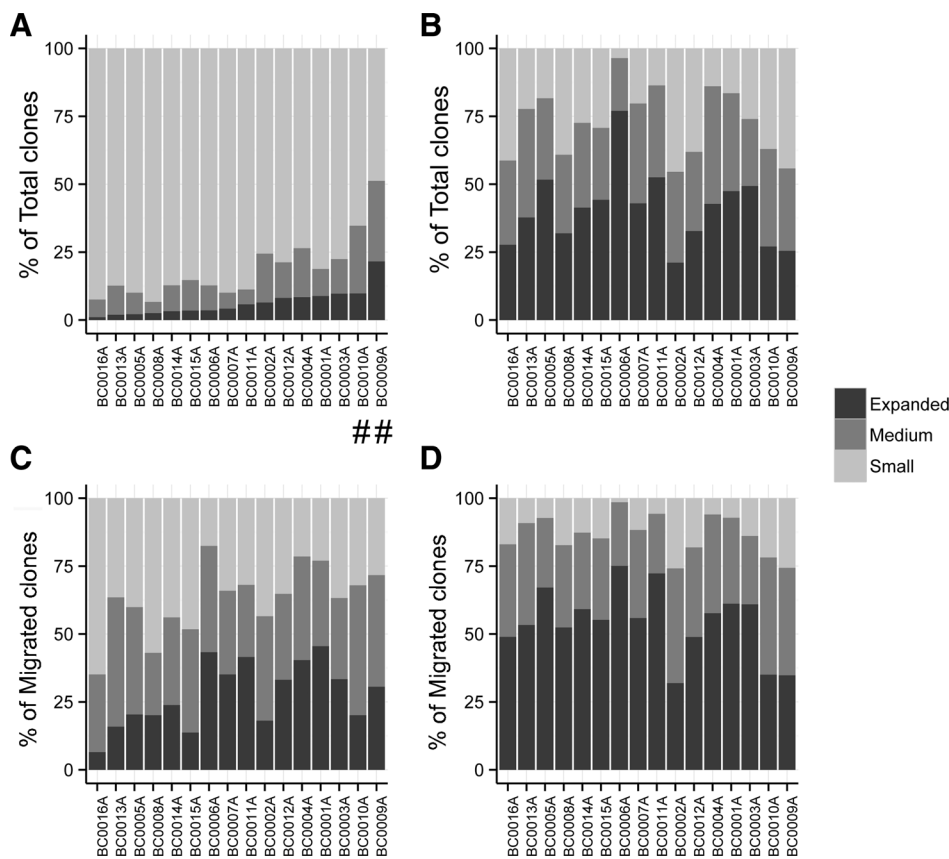
Furthermore, when assessing the clonality of T-cell repertoire in tumors and LNs, we found that most (61.91%–96.42%) T cells in tumors were expanded (>0.1%) or medium-sized (0.01%–0.1%) clones, whereas the small clones (<0.01%) were more prevalent in the LNs (Fig. 3A and B). Large and expanded T-cell clones have activated phenotypes (31), so we infer from our results that the infiltrated T cells in the tumor microenvironment were highly activated and expanded. In contrast, T-cell clonal expansion in the LNs was much lower, where most of the T cells are naïve. Additionally, for the CDR3 sequences identified in both tumors and LNs, which we defined as "migrated clones," we found that their frequencies were significantly higher in tumors than in LNs for all patients except BC0009A, who was node-positive with high LN ratio (LNR; Supplementary Fig. S4). These data are consistent with the hypothesis that T lymphocytes represented by migrated clones are less expanded in the LN and then undergo remarkable expansion after they traffic to the tumor microenvironment, where they encounter and recognize tumor antigens. In some node-positive patients with high LNRs (such as BC0009A), the T lymphocytes may also be activated and expanded in the LNs, perhaps due to more

**Figure 2.**

Shared clones between different tissues. The percentage was calculated by dividing the total clones of each tissue by the shared clones. **A**, The proportion of shared clones between LN and nontumor tissue. **B**, The proportion of shared clones between LN and tumor tissue. \*\*\* $p < 0.001$  according to Mann-Whitney U test.

**Figure 3.**

Percentage of T-cell clones of tumor and LN tissue in different degree of expansion for each patient. Colored bars represent the percentage of T-cell clones in each proportion. (Expanded clone: > 0.1%; medium clone: 0.01%–0.1%; small clone: < 0.01%). **A**, Total T-cell clones of LN tissue. **B**, Total T-cell clones of tumor tissue. **C**, T-cell clones of LN shared with tumor tissue. **D**, T-cell clones of tumor tissue shared with LN tissue. # Node-positive patients with high LNR (>70%). The patients were ordered in sequence of their percentage of expanded clones for the total T cells in the LNs, from the smallest to the largest.



thorough encounter with tumor antigens after tumor metastasis. We also investigated the frequency distribution of migrated T cells versus total T cells and found that significantly more migrated clones were expanded and high-frequency (expanded and large) in both tumors (Fig. 3B and D; Supplementary Fig. S5A) and LNs (Fig. 3 A and C; Supplementary Fig. S5B). This implied that activated but not naïve T cells were more likely to be recruited from the LN, and migrated T cells could be further expanded in the tumor environment, where they could modulate immunologic functions during tumorigenesis.

#### LN positivity correlated with more infiltration of T cells in tumors and expansion in LNs

The LNR, defined as the number of positive LNs (pLN) divided by the number of LNs removed during surgery, provides an independent score for prediction of prognosis and survival (32, 33). We therefore investigated the association among the LNR, number of pLN, degree of infiltration of T cells, and their clonality and expansion.

We found that node-positive tumors had a higher degree of T-cell infiltration than node-negative tumors, though the difference was not significant, perhaps due to the limited number of node-positive samples, and in 3 of 5 only one pLN was detected ( $P = 0.1416$ , Fig. 4A). The difference was more apparent in tumors with higher LNR. The two tumors with LNR above 70% had an infiltration rate of 40% and 30% (defined as the percentage of CD3<sup>+</sup> T cells in the total nucleated cells), respectively (Table 1). To validate this observation, we collected 14 additional tumor samples with high LNR (>50%)

and 6 additional tumor samples from node-negative patients. The two groups shared matched tumor subtypes and grades. Indeed, we found the infiltration ratios of high LNR tumors were significantly higher than those of the node-negative tumors ( $P = 0.00022$ , Fig. 4B).

We also noticed that more expanded T cells were present in the LN with high LNR, compared with node-negative patients (Fig. 3A). To validate this observation, data from another cohort of 49 breast cancer patients were analyzed (Supplementary Table S3). We found node-positive patients had significantly higher T-cell expansion in their LNs, and the increment was even more obvious only taking into account of LNs with high LNR (30% were used here as to include more samples in the group for statistical test, Fig. 4C). Other clinical features, including tumor subtypes and grades, were matched between the node-positive and -negative groups. It implies that the metastatic tumor cells in the LN might enhance activation and expansion of the tumor-associated T cells. We also calculated the *TRB* Pearson coefficient between tumor and LN, indicative of similarity of T-cell repertoire between the two compartments, and found that the T-cell repertoires between tumor and LN were more similar in the high LNR patients (Supplementary Fig. S6A).

#### Similarity of T-cell repertoire between tumors and nontumors affected by tumor subtype

To explore the relationship of T lymphocytes in different tissues, we calculated the Pearson coefficient between each pair of tissues and found that T lymphocytes between tumors and nontumors, as well as between LNs and tumors, were significantly

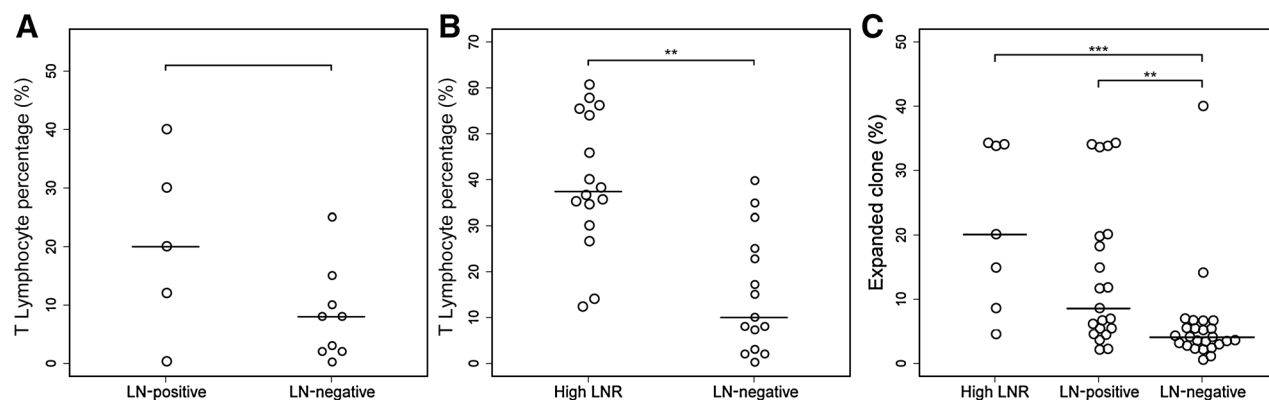


**Figure 4.**

Correlation of node positivity with T lymphocyte ratio in tumor and expansion in LN. **A**, Comparison of infiltration proportion of T lymphocytes in tumor tissue of LN-positive patients and LN-negative patients ( $P = 0.1416$ ). **B**, Comparison of infiltration proportion of T lymphocytes in tumor tissue of patients with high LNR and LN-negative patients ( $P = 0.00022$ ). **C**, Comparison of T-cell expansion in LN for node-negative, node-positive, and high LNR patients (\*,  $P < 0.05$ ; \*\*,  $P < 0.01$ ; \*\*\*,  $P < 0.001$ , according to the Mann-Whitney  $U$  test; LNR, lymph node ratio).

higher than between LNs and nontumors (Supplementary Fig. S6B). In addition, the similarities of T-cell repertoire between tumors and nontumors, as well as LNs and tumors, varied extensively in different patients. To investigate if the diversified intertissue T-cell repertoire similarity among patients was related to breast cancer phenotype, the intertissue correlations among the breast cancer subtypes were compared, and the Pearson coefficients between tumors and nontumors were significantly higher in luminal-like subtype (luminal A and B) than in basal-like subtype ( $P = 0.03596$ , Fig. 5A). Data of the independent validation cohort were also analyzed, but only five basal-like tumors were identified out of 49 patients, which provided insufficient power for statistical test. Therefore, we combined the two cohorts together and demonstrated a significantly higher correlation between luminal-like tumors and paired nontumor tissues ( $P = 0.02017$ , Fig. 5B).

#### Public intratumoral TCR response

The TCR response between individuals for various diseases including cancer can be "public" (found in more than one individual; refs. 23, 24). To examine whether any intratumoral

TCR clones that responded to breast cancer were public, we compared the large and expanded *TRB* amino-acid sequences (>0.01%) from the tumors of multiple patients and filtered the public clones (existing in at least two healthy individuals), with a TCR database collected from peripheral blood of 661 healthy individuals (not published). Thus, we identified 24 TCR amino-acid sequences that were shared by at least 2 patients (Table 2), and the top clone in the list was found in 3 of 16 patients. The frequencies of these public sequences mostly accounted for 0.01% to 1% of the total sequences in an individual. We found that 29.2% (7/24) of public TCRs use *TRB*J2-3 for recombination, which greatly surpassed the frequency of its usage for all the intratumoral TCRs in various patients (10.46%–15.65%), implying the contribution of combinatorial bias to public TCR usage. In addition, some of the public TCRs were recombined by different germline V genes, which further formed variable nucleotide sequences, and eventually encoded the same amino-acid sequences. This clearly illustrates the role of "convergent recombination" in the development of public TCR response (34). Taken together, our data imply that multiple mechanisms are involved in this process.

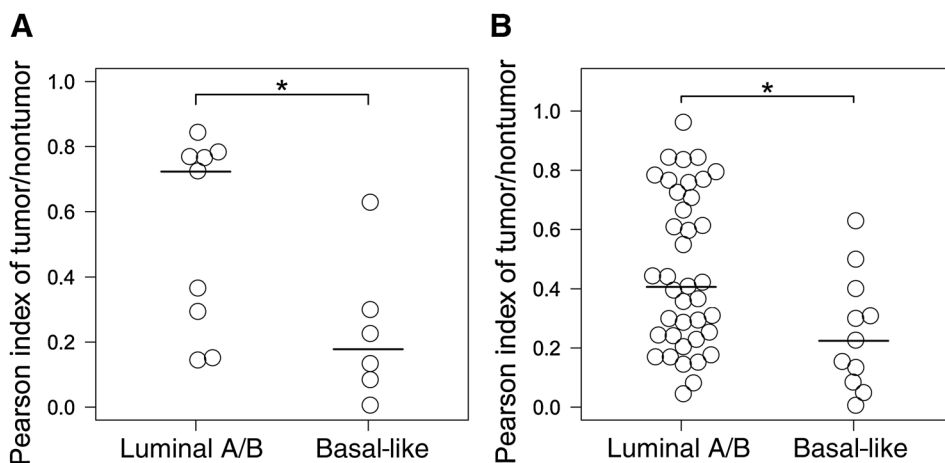


**Figure 5.**

The Pearson correlation coefficients between tumor and nontumor in luminal-like and basal-like breast cancer subtypes. **A**, The comparison in the main cohort. **B**, The comparison combining the main cohort with the validation cohort (\*,  $P < 0.05$  according to the Mann-Whitney  $U$  test).

**Table 2.** Public TRB CDR3 clones among tumor tissues of all 16 patients

Clone_CDR3	Sample number	V gene	J gene	ID (%)
CSARSPGYEQYF	3	TRBV20-1	TRBJ2-7	BC0002A(0.0035) BC0007A(0.0163) BC0012A(0.0196)
CAIESTQAYEQYF	3	TRBV10-3	TRBJ2-7	BC0005A(0.0044) BC0007A(0.0229) BC0009A(0.0200)
CASSLGQSSYGTYF	3	TRBV5-1	TRBJ1-2	BC0002A(0.0038) BC0004A(0.0101) BC0011A(0.0243)
CATSRDSGGLGTTDTQYF	3	TRBV15	TRBJ2-3	BC0002A(0.0006) BC0005A(1.0582) BC0006A(0.0107)
CSVDAGGGNTIYF	2	TRBV29-1	TRBJ1-3	BC0012A(0.0291) BC0013A(0.0481)
CSARVGLAGADTQYF	2	TRBV20-1	TRBJ2-3	BC0005A(0.0134) BC0014A(0.0116)
CASSGTGGSSNQPHF	2	TRBV6-3 TRBV6-2	TRBJ1-5	BC0001A(0.0166) BC0009A(0.0524)
CSVAGTSGRNTGELFF	2	TRBV29-1	TRBJ2-2	BC0013A(0.0160) BC0015A(0.1018)
CSAREIGGGGQPHF	2	TRBV20-1	TRBJ1-5	BC0003A(0.0204) BC0008A(0.0135)
CSASPLAGRETQYF	2	TRBV20-1	TRBJ2-5	BC0004A(0.0131) BC0013A(0.0102)
CSVEEAYEQYF	2	TRBV29-1	TRBJ2-7	BC0005A(0.0453) BC0007A(0.0135)
CSANFRERNSPLHF	2	TRBV20-1	TRBJ1-6	BC0005A(0.8711) BC0006A(0.0107)
CASSLFQGGPSYEQYF	2	TRBV7-8	TRBJ2-7	BC0001A(0.0188) BC0010A(0.0837)
CSASQTDYF	2	TRBV20-1	TRBJ2-3	BC0002A(0.0278) BC0008A(0.0358)
CASSFAASKHYEQYF	2	TRBV12-4 TRBV12-3	TRBJ2-7	BC0016A(0.0152) BC0008A(0.0352)
CSASRRDGTDTQYF	2	TRBV20-1	TRBJ2-3	BC0015A(0.0171) BC0008A(0.0149)
CATSLAGGETQYF	2	TRBV24/OR9-2 TRBV24-1	TRBJ2-5	BC0011A(0.0100) BC0015A(0.1671)
CATSDINEQFF	2	TRBV24/OR9-2 TRBV24-1	TRBJ2-1	BC0002A(0.0123) BC0010A(0.0211)
CAWSPSGGLPQYF	2	TRBV30	TRBJ2-3	BC0005A(0.4246) BC0006A(0.0113)
CATSRENNEQFF	2	TRBV15	TRBJ2-1	BC0003A(0.0113) BC0005A(0.0115)
CSAPGGSGNTIYF	2	TRBV20-1	TRBJ1-3	BC0001A(0.0108) BC0013A(0.0109)
CASSLVGRGDYGYTF	2	TRBV7-2	TRBJ1-2	BC0003A(0.0141)
		TRBV5-1	TRBJ1-2	BC0004A(0.0177)
CASSATGTGANSPLHF	2	TRBV5-1	TRBJ1-6	BC0001A(0.0147)
		TRBV2	TRBJ1-6	BC0003A(0.1580)
CASSTNTDTQYF	2	TRBV12-4 TRBV12-3	TRBJ2-3	BC0010A(0.0182)
		TRBV19	TRBJ2-3	BC0009A(0.0301)

Note: All these clones were filtered with a *TRB* database of 661 healthy individuals.

## Discussion

We have presented here a comprehensive investigation on TCR repertoire for breast cancer. Using IHC and *TRB* CDR3 deep sequencing, we unraveled an unpredicted degree of heterogeneity of T lymphocyte in tumor and other tissues in breast cancer patients. The presence of TILs, especially CD8<sup>+</sup> T cells, correlates with improved clinical prognosis in most of the tumor types (5). With the help of our complete breast cancer sample set, we not only could assess and compare the extent of TILs in different tissues, but also systematically investigated TCR diversity and clonality, and correlated it with tumor molecular subtypes. The characteristics and relationship of TCR repertoire between tumor and adjacent tissues, especially LNs, helped us to assess the process of TIL activation, recruitment, expansion, and selection.

Many studies show that the draining LN is where tumor antigens are first presented to T cells by antigen-presenting cells, which will induce the activation and proliferation of tumor-specific T cells (35–37). Then the proliferating T cells infiltrate the tumor microenvironment by complex mechanisms (38). The tumor mass can also serve as a potential site for T-cell activation (37, 39). Here, we found that T cells in draining LN were more diversified, with fewer large and expanded clones (Fig. 1B; Supplementary Fig. S2), which implied the presence of more naïve cells or unexpanded activated cells. In contrast, TILs had less diversity, with a greater proportion of large and expanded clones (Fig. 1B; Supplementary Fig. S2), which illustrated the universal T-cell activation and proliferation in the tumor microenvironment, where plenty of tumor mass and neoantigens could stimulate the process. Nontumor tissues harbor few T cells, and those present could be tissue-resident memory T cells (TRM; ref. 40) migrating to the nontumor breast

tissue due to historical inflammation or because of minimal migration and the presence of tumor antigens in the nontumor tissues to recruit the T cells.

The relationship between the amount of T cell infiltration into tumors and pLN/LNR has not been reported to date. In our study, we found that node-positive patients tended to have more TILs, and patients with high LNR (>50%) had significantly more TILs than node-negative patients (Fig. 4A and B). More studies are needed to uncover the mechanism underlying this phenomenon. A possible explanation is that enhanced activation and expansion of T lymphocytes by tumor antigens in pLN increases the probability of T cells crossing vasculature and stromal barriers, thereby reaching the tumor site and encountering tumor cells. In addition, the *TRB* repertoire was more similar between tumors and LNs in patients with high LNRs, compared with node-negative patients (Supplementary Fig. S6A). This strongly illustrated the effect of tumor-cell training on the surrounding T lymphocytes, and indicated that many T-cell clones in tumor tissues were tumor reactive.

The correlation between tumor and adjacent nontumors is higher in luminal A/B type breast cancer, whereas it is significantly lower in basal-like type breast cancer (Fig. 5A and B). The heterogeneity of the infiltrated TCR repertoire is shaped and modulated by the variety of neoantigens in the tumor microenvironment. Aberrantly expressed tumor genes derived by their somatic mutations contribute significantly to these tumor neoantigens. The overall mutation rate in luminal A/B breast cancer is the lowest among all the breast cancer subtypes, whereas the mutation rate is higher in the basal-like subtype (34). It is possible that the antigenic microenvironment is more similar between tumor and normal tissues in luminal A/B breast cancer, due to its lower mutation rate, and in turn, it shaped the higher similarity of the TCR repertoire between tumor and nontumor tissue,

compared with basal-like breast cancer. Further studies and evidence are required to support this explanation.

The data on the TCR repertoire used by T cells that infiltrate tumors and neighboring tissues in breast cancer have implications for future diagnoses, monitoring, and predicting prognoses. The identification of tumor-reactive lymphocytes will benefit from the analysis of immune repertoires in tumor microenvironments. Tumor-reactive lymphocytes circulating in the peripheral blood could also serve as potential noninvasive biomarkers to monitor the response of the solid tumor to treatment, track minimal residual disease, and predict relapse. We detected numerous tumor-infiltrated TCR clones in the peripheral blood of the patients before and after surgery (data not shown). However, whether the dynamic change of the frequency of these TCR clones after surgery and further treatment has clinical implications still warrants prospective studies and long-term follow-up of patients. On the other hand, tumor-reactive lymphocytes as direct antitumor weapons in immunotherapy can be tracked and monitored in the ACT process, by deep-sequencing and immune repertoire analysis. In summary, the comprehensive analysis of the characteristic TCR repertoire in breast cancer has depicted a landscape of immunosurveillance and interactions with tumor cells, as well as the relationship of TCR repertoires to various clinical features.

## References

- Qian BZ, Pollard JW. Macrophage diversity enhances tumor progression and metastasis. *Cell* 2010;141:39–51.
- Motz GT, Coukos G. Deciphering and reversing tumor immune suppression. *Immunity* 2013;39:61–73.
- Lindau D, Gielen P, Kroesen M, Wesseling P, Adema GJ. The immunosuppressive tumour network: myeloid-derived suppressor cells, regulatory T cells and natural killer T cells. *Immunology* 2013;138:105–15.
- Dunn GP, Bruce AT, Ikeda H, Old LJ, Schreiber RD. Cancer immunoediting: from immunosurveillance to tumor escape. *Nat Immunol* 2002;3:991–8.
- Gooden MJ, de Bock GH, Leffers N, Daemen T, Nijman HW. The prognostic influence of tumour-infiltrating lymphocytes in cancer: a systematic review with meta-analysis. *Br J Cancer* 2011;105:93–103.
- Hwang WT, Adams SF, Tahirovic E, Hagemann IS, Coukos G. Prognostic significance of tumor-infiltrating T cells in ovarian cancer: a meta-analysis. *Gynecol Oncol* 2012;124:192–8.
- Piersma SJ, Jordanova ES, van Poelgeest MI, Kwappenberg KM, van der Hulst JM, Drijfhout JW, et al. High number of intraepithelial CD8+ tumor-infiltrating lymphocytes is associated with the absence of lymph node metastases in patients with large early-stage cervical cancer. *Cancer Res* 2007;67:354–61.
- Huh JW, Lee JH, Kim HR. Prognostic significance of tumor-infiltrating lymphocytes for patients with colorectal cancer. *Arch Surg* 2012;147:366–72.
- Ohtani H. Focus on TILs: prognostic significance of tumor infiltrating lymphocytes in human colorectal cancer. *Cancer Immunity* 2007;7:4.
- Deschoolmeester V, Baay M, Van Marck E, Weyler J, Vermeulen P, Lardon F, et al. Tumor infiltrating lymphocytes: an intriguing player in the survival of colorectal cancer patients. *BMC Immunol* 2010;11:19.
- Ma C, Zhang Q, Ye J, Wang F, Zhang Y, Wevers E, et al. Tumor-infiltrating gamma delta T lymphocytes predict clinical outcome in human breast cancer. *J Immunol* 2012;189:5029–36.
- Adams S, Gray RJ, Demaria S, Goldstein L, Perez EA, Shulman LN, et al. Prognostic value of tumor-infiltrating lymphocytes in triple-negative breast cancers from two phase III randomized adjuvant breast cancer trials: ECOG 2197 and ECOG 1199. *J Clin Oncol* 2014;32:2959–67.
- Liu S, Lachapelle J, Leung S, Gao D, Foulkes WD, Nielsen TO. CD8+ lymphocyte infiltration is an independent favorable prognostic indicator in basal-like breast cancer. *Breast Cancer Res* 2012;14:R48.
- Rathore AS, Kumar S, Konwar R, Srivastava AN, Makker A, Goel MM. Presence of CD3+ tumor infiltrating lymphocytes is significantly associated with good prognosis in infiltrating ductal carcinoma of breast. *Indian J Cancer* 2013;50:239–44.
- Restifo NP, Dudley ME, Rosenberg SA. Adoptive immunotherapy for cancer: harnessing the T cell response. *Nat Rev Immunol* 2012;12:269–81.
- Rosenberg SA, Yang JC, Sherry RM, Kammula US, Hughes MS, Phan GQ, et al. Durable complete responses in heavily pretreated patients with metastatic melanoma using T-cell transfer immunotherapy. *Clin Cancer Res* 2011;17:4550–7.
- Hodi FS, O'Day SJ, McDermott DF, Weber RW, Sosman JA, Haanen JB, et al. Improved survival with ipilimumab in patients with metastatic melanoma. *N Engl J Med* 2010;363:711–23.
- Topalian SL, Hodi FS, Brahmer JR, Gettinger SN, Smith DC, McDermott DF, et al. Safety, activity, and immune correlates of anti-PD-1 antibody in cancer. *N Engl J Med* 2012;366:2443–54.
- Gerlinger M, Quezada SA, Peggs KS, Furness AJ, Fisher R, Marafioti T, et al. Ultra-deep T cell receptor sequencing reveals the complexity and intratumour heterogeneity of T cell clones in renal cell carcinomas. *J Pathol* 2013;231:424–32.
- Emerson RO, Sherwood AM, Rieder MJ, Guenther J, Williamson DW, Carlson CS, et al. High-throughput sequencing of T-cell receptors reveals a homogeneous repertoire of tumour-infiltrating lymphocytes in ovarian cancer. *J Pathol* 2013;231:433–40.
- Hindley JP, Ferreira C, Jones E, Lauder SN, Ladell K, Wynn KK, et al. Analysis of the T-cell receptor repertoires of tumor-infiltrating conventional and regulatory T cells reveals no evidence for conversion in carcinogen-induced tumors. *Cancer Res* 2011;71:736–46.
- Soliman H, Khalil F, Antonia S. PD-L1 expression is increased in a subset of basal type breast cancer cells. *PLoS ONE* 2014;9:e88557.
- Venturi V, Price DA, Douek DC, Davenport MP. The molecular basis for public T-cell responses? *Nat Rev Immunol* 2008;8:231–8.
- Miles JJ, Douek DC, Price DA. Bias in the alpha beta T-cell repertoire: implications for disease pathogenesis and vaccination. *Immunol Cell Biol* 2011;89:375–87.
- Onitilo AA, Engel JM, Greenlee RT, Mukesh BN. Breast cancer subtypes based on ER/PR and Her2 expression: comparison of clinicopathologic features and survival. *Clin Med Res* 2009;7:4–13.

## Disclosure of Potential Conflicts of Interest

No potential conflicts of interest were disclosed.

## Authors' Contributions

**Conception and design:** T. Wang, R. Zhang, X. Zhang, X. Xu, L. Wang, X. Liu  
**Development of methodology:** C. Wang, J. Wu, J. Liu, R. Zhang, X. Zeng, X. Zhang, X. Liu

**Acquisition of data (provided animals, acquired and managed patients, provided facilities, etc.):** T. Wang, J. Wu, C. He, J. Liu, Y. Li

**Analysis and interpretation of data (e.g., statistical analysis, biostatistics, computational analysis):** C. Wang, J. Wu, W. Zhang, H. Cao, X. Liu

**Writing, review, and/or revision of the manuscript:** C. Wang, J. Wu, Y. Lv, X. Zhang, C. Huang, X. Liu

**Administrative, technical, or material support (i.e., reporting or organizing data, constructing databases):** X. Zeng, X. Zhang, X. Xu

**Study supervision:** X. Zhang, X. Xu

## Acknowledgments

This work was supported by the National Natural Science Fund (81272899, 81672593, 30973463, and 81470120), the Shaanxi Fund (2013K12-03-03 and 2014JM4087), the Xi'an Fund (SF1323(3)), and Discipline Booster Plan of the Xijing Hospital (XJZT12Z07 and 2014JM4087).

The costs of publication of this article were defrayed in part by the payment of page charges. This article must therefore be hereby marked *advertisement* in accordance with 18 U.S.C. Section 1734 solely to indicate this fact.

Received May 18, 2016; revised November 15, 2016; accepted December 5, 2016; published OnlineFirst December 30, 2016.



26. Robins HS, Campregher PV, Srivastava SK, Wachter A, Turtle CJ, Khsai O, et al. Comprehensive assessment of T-cell receptor beta-chain diversity in alphabeta T cells. *Blood* 2009;114:4099–107.
27. Boyd SD, Marshall EL, Merker JD, Maniar JM, Zhang LN, Sahaf B, et al. Measurement and clinical monitoring of human lymphocyte clonality by massively parallel VDJ pyrosequencing. *Sci Translat Med* 2009;1:12ra23.
28. Wang C, Sanders CM, Yang Q, Schroeder HWJr, Wang E, Babrzadeh F, et al. High throughput sequencing reveals a complex pattern of dynamic interrelationships among human T cell subsets. *Proc Natl Acad Sci USA* 2010;107:1518–23.
29. Zhang W, Du Y, Su Z, Wang C, Zeng X, Zhang R, et al. IMonitor: a robust pipeline for TCR and BCR repertoire analysis. *Genetics* 2015;201:459–72.
30. Kaplinsky J, Li A, Sun A, Coffre M, Koralov SB, Arnaout R. Antibody repertoire deep sequencing reveals antigen-independent selection in maturing B cells. *Proc Natl Acad Sci USA* 2014;111:E2622–9.
31. Putintseva EV, Britanova OV, Staroverov DB, Merzlyak EM, Turchaninova MA, Shugay M, et al. Mother and child T cell receptor repertoires: deep profiling study. *Front Immunol* 2013;4:463.
32. Van Belle V, Van Calster B, Wildiers H, Van Huffel S, Neven P. Lymph node ratio better predicts disease-free survival in node-positive breast cancer than the number of positive lymph nodes. *J Clin Oncol* 2009;27:e150–1; author reply e2.
33. Vinh-Hung V, Verkooijen HM, Fioretta G, Neyroud-Caspar I, Rapiti E, Vlastos G, et al. Lymph node ratio as an alternative to pN staging in node-positive breast cancer. *J Clin Oncol* 2009;27:1062–8.
34. Comprehensive molecular portraits of human breast tumours. *Nature* 2012;490:61–70.
35. Yoon H, Legge KL, Sung SS, Braciale TJ. Sequential activation of CD8+ T cells in the draining lymph nodes in response to pulmonary virus infection. *J Immunol* 2007;179:391–9.
36. Mempel TR, Henrickson SE, Von Andrian UH. T-cell priming by dendritic cells in lymph nodes occurs in three distinct phases. *Nature* 2004;427:154–9.
37. Bai XF, Gao JX, Liu J, Wen J, Zheng P, Liu Y. On the site and mode of antigen presentation for the initiation of clonal expansion of CD8 T cells specific for a natural tumor antigen. *Cancer Res* 2001;61:6860–7.
38. Marelli-Berg FM, Cannella L, Dazzi F, Miranda V. The highway code of T cell trafficking. *J Pathol* 2008;214:179–89.
39. Thompson ED, Enriquez HL, Fu YX, Engelhard VH. Tumor masses support naive T cell infiltration, activation, and differentiation into effectors. *J Exp Med* 2010;207:1791–804.
40. Shin H, Iwasaki A. Tissue-resident memory T cells. *Immunol Rev* 2013;255:165–81.

# Cancer Immunology Research

## The Different T-cell Receptor Repertoires in Breast Cancer Tumors, Draining Lymph Nodes, and Adjacent Tissues

Ting Wang, Changxi Wang, Jinghua Wu, et al.

*Cancer Immunol Res* Published OnlineFirst December 30, 2016.

<b>Updated version</b>	Access the most recent version of this article at: doi: <a href="https://doi.org/10.1158/2326-6066.CIR-16-0107">10.1158/2326-6066.CIR-16-0107</a>
<b>Supplementary Material</b>	Access the most recent supplemental material at: <a href="http://cancerimmunolres.aacrjournals.org/content/suppl/2016/12/30/2326-6066.CIR-16-0107.DC1">http://cancerimmunolres.aacrjournals.org/content/suppl/2016/12/30/2326-6066.CIR-16-0107.DC1</a>

**E-mail alerts** [Sign up to receive free email-alerts](#) related to this article or journal.

**Reprints and Subscriptions** To order reprints of this article or to subscribe to the journal, contact the AACR Publications Department at [pubs@aacr.org](mailto:pubs@aacr.org).

**Permissions** To request permission to re-use all or part of this article, use this link <http://cancerimmunolres.aacrjournals.org/content/early/2017/01/16/2326-6066.CIR-16-0107>. Click on "Request Permissions" which will take you to the Copyright Clearance Center's (CCC) Rightslink site.